

# MIM-Based Generative Adversarial Networks and Its Application on Anomaly Detection

Rui She, Pingyi Fan, *Senior Member, IEEE*

## Abstract

In terms of Generative Adversarial Networks (GANs), the information metric to discriminate the generative data and the real data, lies in the key point of generation efficiency, which plays an important role in GAN-based applications, especially in anomaly detection. As for the original GAN, the information metric based on Kullback-Leibler (KL) divergence has limitations on rare events generation and training performance for adversarial networks. Therefore, it is significant to investigate the metrics used in GANs to improve the generation ability as well as bring gains in the training process. In this paper, we adopt the exponential form, referred from the Message Importance Measure (MIM), to replace the logarithm form of the original GAN. This approach named MIM-based GAN, has dominant performance on training process and rare events generation. Specifically, we first discuss the characteristics of training process in this approach. Moreover, we also analyze its advantages on generating rare events in theory. In addition, we do simulations on the datasets of MNIST and ODDS to see that the MIM-based GAN achieves state-of-the-art performance on anomaly detection compared with some classical GANs.

## Index Terms

Generative Adversarial Networks, Information Metric, Kullback-Leibler (KL) Divergence, Rare Events Generation, Anomaly Detection

## I. INTRODUCTION

In order to generate deceptive fake data, Generative Adversarial Networks (GANs) are proposed as a kind of efficient approach [1]. Especially, complex or high-dimensional distributions are handled pretty well by GANs [2], [3]. Actually, the core idea of GANs is to generate samples whose distribution approximates

R. She and P. Fan were supported by the National Natural Science Foundation of China (NSFC) No. 61771283.

R. She and P. Fan are with Beijing National Research Center for Information Science and Technology and the Department of Electronic Engineering, Tsinghua University, Beijing, 100084, China (e-mail: sher15@mails.tsinghua.edu.cn; fpy@tsinghua.edu.cn).

the target distribution as much as possible. In practice, GANs are applied in many scenarios [4]–[8], such as images reconstruction, autonomous driving models, and samples augmentation. In theory, the framework of GANs consists of a generator network and a discriminator network, which respectively minimizes and maximizes the distinction between the real data distribution and the generated distribution. In this case, the information distance (which is Jensen-Shannon divergence in the original GAN) plays a vital role in the generative adversarial process. On one hand, the performance of training process depends on the information distance. On the other hand, the efficiency of generative data (especially for rare events data) is related to this metric. Therefore, it is worth investigating the information distance and its corresponding objective function of GANs to improve the training process and GAN-based applications such as anomaly detection.

#### A. Different information distances for GANs

Considering the information distance choice of GANs, there are some literatures discussing how the different distances make impacts on the optimization of objective functions in the generative process. In terms of the original GAN, it optimizes the Jensen-Shannon divergence (which is based on Kullback-Leibler (KL) divergence) to generate samples. Similar to the original generative model, the affine projected GAN (or AffGAN for short) is also discussed to minimize the KL divergence between the two distributions (namely, the real data distribution and the generative one), which is suitable for Maximum a Posterior (MAP) inference with respect to image super-resolution [9]. However, there exists faultiness for KL divergence as a metric in the objective function of GANs, which performs in training stability and efficiency. To make up for this, some other information distances are considered to replace the original KL divergence as follows.

As a kind of improved GAN, Energy-Based Generative Adversarial Network (EBGAN), based on the total variation (a kind of information distance), allocates lower energies to the adjacent regions of the real data manifold and larger energies to the rest regions. Compared with the original GAN, the EBGAN performs more stable in the training process [10]. Moreover, to overcome the vanishing gradients problem caused by the loss function of the original GAN, Least Squares Generative Adversarial Networks (LSGAN) is proposed, which is to minimize the Pearson  $\chi^2$  divergence as the objective function [11]. Another distance, Chi-Squared distance, is also used to design the Fisher GAN which constrains the second order moments of the critic and leads to train the adversarial networks in a stable and efficient way [12]. To extend GANs into a general way,  $f$ -divergence is discussed to train generative models where the benefits

of different information distances belonging to  $f$ -divergence are investigated with respect to the training complexity and the quality [13]. In addition, Wasserstein-GAN (WGAN) is proposed to estimate Earth Mover distance (EM distance) continuously, which overcomes the problem of GANs, that is to make a training balance between the discriminator and the generator. Furthermore, an improved WGAN with gradient penalty (named WGAN-GP) is also introduced to enforce the Lipschitz constraint, which enables a more stable training process without any hyper-parameter tuning [14], [15].

In brief, it is a popular research direction to introduce a promising information distance into GANs to see whether there exist performance gains on training process.

### *B. Generative efficiency for rare events*

Anomaly detection is a common problem with real-world significance [16]–[18]. Inspired by the success of neural networks, GANs are considered as an efficient approach to detect anomalies which are regarded as rare events from the perspective of occurrence probability. Particularly, the original GAN has played great roles in anomalous natural and medical images detection [19], [20].

In terms of the anomaly detection with GANs, the method is to regard the samples as anomalies depending on if the appropriate representations of samples in the latent space of generator are found. Specifically, the generator learns an approximate distribution of the training data, in which there are more normal events (hardly ever with anomalies). Thus, for a normal testing sample, it is probable to find a point in the latent space of GANs similar to this one, while for an anomalous sample it is not. Based on this idea, there exist works using GANs in anomaly detection as follows [21]–[23].

A method called AnoGAN using normal data to train the original GAN [21], defines an anomaly score to distinguish the generative samples (namely normal samples) and the anomalous samples. Moreover, another similar method learns two generators by training a conditional GAN to reconstruct normal frames (with low reconstruction loss) and rare frames (with high reconstruction loss) [24]. Besides, an unsupervised feature learning framework, Bidirectional Generative Adversarial Networks (BiGAN) is also proposed to train the networks with normal data and combine the reconstruction loss and discriminator loss as the score function to detect anomalies [25]. Furthermore, other GAN-based anomaly detection approaches such as Generative Adversarial Active Learning (GAAL) and fast AnoGAN (or f-AnoGAN) are designed by making use of the prior information during the adversarial training process [4], [26].

Moreover, the discriminator to distinguish the real samples and fake ones is also applied reasonably to detecting anomalies. In particular, once the training process is converged, the discriminator can not cope

with the testing data that is unlike the training data (which corresponds to the anomalous data) [27], [28]. As a result, it is feasible to combine the discriminator and generator of GANs to detect anomalies.

However, since the rare events (including anomalies) play a small part in the whole dataset, the generative data more likely belongs to the main part of normal data rather than small probability data. In terms of the original GAN, the proportion of rare events in the objective function is not large enough compared with that for normal events, which makes an effect on rare events generation.

In addition, as for the original GAN, there exist drawbacks in convergence rate, sensitivity and stability of training process. Besides, there are few literatures to investigate the improvements for objective functions (related to information distances) from the perspective of rare events generation, which is also beneficial for GAN-based anomaly detection. Therefore, we have an opportunity to investigate a new information metric to improve the original GAN-based rare events generation and anomaly detection.

In this work, we introduce the idea of Message Importance Measure (MIM) into the GANs and propose a MIM-based GAN method to detect anomalies. In this case, there are improvements in the objective function for training process and rare events generation. Furthermore, experiments on real datasets are taken to compare our method with other classical methods.

### *C. Contributions and organization*

The main contributions of this paper are summarized as follows:

- At first, the core idea of MIM is introduced into the objective function of GANs to construct a new kind of GAN model, i. e. MIM-based GAN, which is used in the context of learning distributions. As well, some characteristics of this GAN are also discussed.
- Then, the proposed MIM-based GAN highlights the proportion of rare events in the objective function, which reveals its advantages on rare events generation in theory.
- At last, compared with conventional GANs, the MIM-based GAN performs better in anomaly detection. Specifically, the experiments (based on artificial dataset and real datasets) are designed to intuitively show the different performance on the results of detection.

In addition, the organization of the rest part is provided as follows. In Section II, we propose the MIM-based GAN by resorting to the idea of MIM and discuss its major properties in the training process. In Section III, we theoretically analyze the effect of rare events on generators and discuss the GAN-based anomaly detection. Section IV design experiments to compare different GANs (including MIM-based

GAN, original GAN, LSGAN and WGAN) in the anomaly detection. Finally, we conclude the works in the Section V.

## II. MODEL OF MIM-BASED GAN

### A. Overview of GANs

In terms of GANs, the essential idea is to train an optimal couple of artificial neural networks, namely, discriminator and generator, to generate the data whose distribution approximates the real data distribution. To do this, the objective functions of GANs play vital roles in the two-player optimization game between the discriminator and generator. In fact, there exists a general form of objective function optimization for GANs, which is described as

$$\min_G \max_D L(D, G), \quad (1)$$

where  $L(D, G)$  denotes the objective function given by

$$\begin{aligned} L(D, G) &= \mathbb{E}_{\mathbf{x} \sim \mathbb{P}}[f(D(\mathbf{x}))] + \mathbb{E}_{\mathbf{z} \sim \mathbb{P}_z}[g(D(G(\mathbf{z})))] \\ &= \mathbb{E}_{\mathbf{x} \sim \mathbb{P}}[f(D(\mathbf{x}))] + \mathbb{E}_{\mathbf{x} \sim \mathbb{P}_{g\theta}}[g(D(\mathbf{x}))], \end{aligned} \quad (2)$$

in which  $f(\cdot)$  and  $g(\cdot)$  are functions,  $D$  is the discriminator,  $G$  is the generator ( $D$  and  $G$  are both represented by neural networks),  $\mathbf{x}$  and  $\mathbf{z}$  denote the input for  $D$  and  $G$  respectively, as well as  $\mathbb{P}$ ,  $\mathbb{P}_{g\theta}$  and  $\mathbb{P}_z$  are distributions for real data, generative data and input data of generator.

TABLE I  
SUMMARY OF GANs BASED ON THE GENERAL FORM OF OBJECTIVE FUNCTIONS

Type of GANs	Objective Function Optimization	Key Points
Original GAN [1]	$\min_G \max_D \{ \mathbb{E}_{\mathbf{x} \sim \mathbb{P}}[\ln D(\mathbf{x})] + \mathbb{E}_{\mathbf{z} \sim \mathbb{P}_z}[\ln(1 - D(G(\mathbf{z})))] \}$ $\Leftrightarrow$ $\max_G \min_D \left\{ \mathbb{E}_{\mathbf{x} \sim \mathbb{P}} \left[ \ln \left( \frac{1}{D(\mathbf{x})} \right) \right] + \mathbb{E}_{\mathbf{z} \sim \mathbb{P}_z} \left[ \ln \left( \frac{1}{1 - D(G(\mathbf{z}))} \right) \right] \right\}$	<ul style="list-style-type: none"> <li>corresponding functions in Eq. (2):  <math>f(u) = \ln(u)</math>, <math>g(u) = \ln(1 - u)</math>,  or <math>f(u) = -\ln(\frac{1}{u})</math>, <math>g(u) = -\ln(\frac{1}{1-u})</math>.</li> </ul>
Wasserstein GAN [14]	$\min_G \max_D \left\{ \sup_{\ D\ _L \leq 1} \{ \mathbb{E}_{\mathbf{x} \sim \mathbb{P}}[D(\mathbf{x})] - \mathbb{E}_{\mathbf{z} \sim \mathbb{P}_z}[D(G(\mathbf{z}))] \} \right\},$ <p>where <math>\ \cdot\ _L \leq 1</math> denotes 1-Lipschitz constraint condition.</p>	<ul style="list-style-type: none"> <li>corresponding functions in Eq. (2):  <math>f(u) = u</math> and <math>g(u) = -u</math>.</li> </ul>
LSGAN [11]	$\max_G \min_D \left\{ \frac{1}{2} \mathbb{E}_{\mathbf{x} \sim \mathbb{P}}[(D(\mathbf{x}) - 1)^2] + \frac{1}{2} \mathbb{E}_{\mathbf{z} \sim \mathbb{P}_z}[(D(G(\mathbf{z})))^2] \right\}$	<ul style="list-style-type: none"> <li>corresponding functions in Eq. (2):  <math>f(u) = -\frac{1}{2}(u - 1)^2</math> and <math>g(u) = -\frac{1}{2}u^2</math>.</li> </ul>
MIM-based GAN [Ours]	$\max_G \min_D \{ \mathbb{E}_{\mathbf{x} \sim \mathbb{P}}[\exp(1 - D(\mathbf{x}))] + \mathbb{E}_{\mathbf{z} \sim \mathbb{P}_z}[\exp(D(G(\mathbf{z})))] \}$	<ul style="list-style-type: none"> <li>corresponding functions in Eq. (2):  <math>f(u) = -\exp(1 - u)</math> and <math>g(u) = -\exp(u)</math>.</li> </ul>

## B. MIM-based GAN and Corresponding Characteristics

According to the comparison for MIM and Shannon entropy [29]–[31], it is known that the exponential function used to replace the logarithmic function, has more positive impacts on the rare events processing from the viewpoint of information metrics. Furthermore, based on the exponential function, an information distance, Message Identification (M-I) divergence is proposed to gain the greater effect of amplification on detecting outliers than Kullback-Leibler (KL) divergence (which is based on logarithmic function) [32]. As a result, exponential function with different properties from logarithmic function makes differences on information characterization. In this regard, there may exist potential advantages to introduce exponential function into the original GAN which incorporates the logarithmic function in the objective function.

By virtue of the essential idea of MIM and the convexity of exponential function, we have the modified objective function of GANs as follows

$$\begin{aligned} L_{\text{MIM}}(D, G) &= \mathbb{E}_{\mathbf{x} \sim \mathbb{P}}[\exp(1 - D(\mathbf{x}))] + \mathbb{E}_{\mathbf{z} \sim \mathbb{P}_z}[\exp(D(G(\mathbf{z})))] \\ &= \mathbb{E}_{\mathbf{x} \sim \mathbb{P}}[\exp(1 - D(\mathbf{x}))] + \mathbb{E}_{\mathbf{x} \sim \mathbb{P}_{g\theta}}[\exp(D(\mathbf{x}))], \end{aligned} \quad (3)$$

where the notations (including  $D$ ,  $G$ ,  $\mathbf{x}$ ,  $\mathbf{z}$ ,  $\mathbb{P}$ ,  $\mathbb{P}_{g\theta}$  and  $\mathbb{P}_z$ ) are the same as those in Eq. (2).

Similar to the original GAN, the modified objection function Eq. (3) also plays the two-player optimization game with respect to  $D$  and  $G$  as follows

$$\max_G \min_D L_{\text{MIM}}(D, G), \quad (4)$$

and the corresponding adversarial networks are referred to as *MIM-based GAN*. Essentially, the goal of the MIM-based GAN is to train an optimal couple of discriminator and generator to learn the real data distribution, which is as same as that in the original GAN. In particular, the principle of MIM-based GAN are detailed as follows.

On one hand, the network of discriminator  $D$  is designed to assign the real label (usually “1”) and fake label (usually “0”) to the real data and generative data (from the generator  $G$ ). In this case, the input pairs for  $D$  consist of data (namely real data and generative data) and labels (containing real labels and fake labels). On the other hand, the network of generator  $G$  tends to output imitative data more like the real data, whose goal is to deceive the discriminator. In other words, the discriminator  $D$  is misled by the generator  $G$  to make the similar decision for the generative data and real data. In this case, the input pairs of  $G$  are data  $\mathbf{z}$  (randomly drawn from a latent space) and real labels. Furthermore, the loss functions of  $D$  and  $G$  are given by Eq. (4) which leads the two networks to update their weight parameters by means

of back propagation. Finally, by selecting neural networks structures for  $D$  and  $G$ , the training process of MIM-based GAN is completed.

Then, some fundamental characteristics of MIM-based GAN are discussed as follows.

1) *Optimality of  $\mathbb{P} = \mathbb{P}_{g_\theta}$ :*

Given a generator  $G$ , we investigate the optimal discriminator  $D$  as follows.

**Lemma 1.** *For a fixed generator  $g_\theta$  in the MIM-based GAN, the optimal discriminator  $D$  is given by*

$$D_{\text{MIM}}^*(\mathbf{x}) = \frac{1}{2} + \frac{1}{2} \ln \frac{P(\mathbf{x})}{P_{g_\theta}(\mathbf{x})}, \quad (5)$$

where  $P$  and  $P_{g_\theta}$  are densities of the distributions  $\mathbb{P}$  and  $\mathbb{P}_{g_\theta}$ .

*Proof.* Considering the training criterion of discriminator  $D$  (with a given generator  $g_\theta$ ), we just minimize

$$L_{\text{MIM}}(D, G) = \int_{\mathbf{x}} [P(\mathbf{x}) \exp(1 - D(\mathbf{x})) + P_{g_\theta}(\mathbf{x}) \exp(D(\mathbf{x}))] d\mathbf{x}, \quad (6)$$

and the corresponding solution is the optimal  $D$ .

As for a function  $f(u) = a \exp(1 - u) + b \exp(u)$  ( $a > 0, b > 0$ ), we have the solution  $u = \frac{1}{2} + \ln\left(\frac{a}{b}\right)$  achieving  $\frac{\partial f(u)}{\partial u} = -a \exp(1 - u) + b \exp(u) = 0$ . Besides, due to the fact that the second order derivative  $\frac{\partial^2 f(u)}{\partial u^2} = a \exp(1 - u) + b \exp(u) > 0$ , implying the convexity of  $f(u)$ , we have the solution  $u = \frac{1}{2} + \ln\left(\frac{a}{b}\right)$  achieve the minimum value of  $f(u)$ , which concludes the proof.  $\square$

By substituting the optimal discriminator  $D_{\text{MIM}}^*$  into  $L_{\text{MIM}}(D, G)$  (with any given generator  $G$ ), we have

$$\begin{aligned} & L_{\text{MIM}}(D = D_{\text{MIM}}^*, G) \\ &= \mathbb{E}_{\mathbf{x} \sim \mathbb{P}} [\exp(1 - D_{\text{MIM}}^*(\mathbf{x}))] + \mathbb{E}_{\mathbf{x} \sim \mathbb{P}_{g_\theta}} [\exp(D_{\text{MIM}}^*(\mathbf{x}))] \\ &= \mathbb{E}_{\mathbf{x} \sim \mathbb{P}} \left[ \exp \left( \frac{1}{2} + \ln \left( \frac{P(\mathbf{x})}{P_{g_\theta}(\mathbf{x})} \right)^{-\frac{1}{2}} \right) \right] + \mathbb{E}_{\mathbf{x} \sim \mathbb{P}_{g_\theta}} \left[ \exp \left( \frac{1}{2} + \ln \left( \frac{P(\mathbf{x})}{P_{g_\theta}(\mathbf{x})} \right)^{\frac{1}{2}} \right) \right] \\ &= \sqrt{e} \left\{ \mathbb{E}_{\mathbf{x} \sim \mathbb{P}} \left[ \left( \frac{P(\mathbf{x})}{P_{g_\theta}(\mathbf{x})} \right)^{-\frac{1}{2}} \right] + \mathbb{E}_{\mathbf{x} \sim \mathbb{P}_{g_\theta}} \left[ \left( \frac{P_{g_\theta}(\mathbf{x})}{P(\mathbf{x})} \right)^{-\frac{1}{2}} \right] \right\}. \end{aligned} \quad (7)$$

**Proposition 1.** *As for the MIM-based GAN, the optimal solution of equivalent objective function with the optimal discriminator, i.e.  $L_{\text{MIM}}(D = D_{\text{MIM}}^*, G)$  (mentioned in Eq. (7)), is achieved if and only if  $\mathbb{P} = \mathbb{P}_{g_\theta}$ , where  $L_{\text{MIM}}(D = D_{\text{MIM}}^*, G)$  reaches the maximum value  $2\sqrt{e}$ .*

*Proof.* In the case  $\mathbb{P} = \mathbb{P}_{g_\theta}$  (implying  $D_{\text{MIM}}^*(\mathbf{x}) = \frac{1}{2}$ ), we have the value of Eq. (7) as  $L_{\text{MIM}}(D = \frac{1}{2}, G) = \sqrt{e}(1 + 1) = 2\sqrt{e}$ . This is the maximum value of  $L_{\text{MIM}}(D = D_{\text{MIM}}^*, G)$ , reached at the point  $\mathbb{P} = \mathbb{P}_{g_\theta}$ . According to the expression of Eq. (7), we have the equivalent formulation as follows

$$\begin{aligned} & \max_{g_\theta} L_{\text{MIM}}(D = D_{\text{MIM}}^*, G) \\ & \Leftrightarrow \max_{g_\theta} \sqrt{e} \left\{ \ln \mathbb{E}_{\mathbf{x} \sim \mathbb{P}} \left[ \left( \frac{P(\mathbf{x})}{P_{g_\theta}(\mathbf{x})} \right)^{-\frac{1}{2}} \right] + \ln \mathbb{E}_{\mathbf{x} \sim \mathbb{P}_{g_\theta}} \left[ \left( \frac{P_{g_\theta}(\mathbf{x})}{P(\mathbf{x})} \right)^{-\frac{1}{2}} \right] \right\}. \end{aligned} \quad (8)$$

Then, it is not difficult to see that

$$\max_{g_\theta} L_{\text{MIM}}(D = D_{\text{MIM}}^*, G) \Leftrightarrow \min_{g_\theta} \frac{\sqrt{e}}{2} \left\{ R_{\alpha=\frac{1}{2}}(\mathbb{P} \parallel \mathbb{P}_{g_\theta}) + R_{\alpha=\frac{1}{2}}(\mathbb{P}_{g_\theta} \parallel \mathbb{P}) \right\}, \quad (9)$$

where  $R_{\alpha=\frac{1}{2}}(\cdot)$  is the Renyi divergence (whose parameter satisfies  $\alpha = \frac{1}{2}$ ) which is defined as

$$R_\alpha(\mathbb{P} \parallel \mathbb{Q}) = \frac{1}{\alpha - 1} \ln \left\{ \mathbb{E}_{\mathbf{x} \sim \mathbb{P}} \left[ \left( \frac{P(\mathbf{x})}{Q(\mathbf{x})} \right)^{\alpha-1} \right] \right\}, \quad (\alpha > 0, \alpha \neq 1). \quad (10)$$

Due to the fact that Renyi divergence (with parameter  $\alpha = \frac{1}{2}$ ) reaches the minimum only when two distributions are equal, it is readily seen that  $2\sqrt{e}$  is the global maximum of  $L_{\text{MIM}}(D = D_{\text{MIM}}^*, G)$  and the corresponding solution is  $\mathbb{P} = \mathbb{P}_{g_\theta}$ , that is to say, the generative model replicates the real data.  $\square$

**Remark 1.** *Similar to the original GAN, there exists a training equilibrium for the two-player optimization game in the MIM-based GAN. In this regard, the global optimality lies at the point of  $\mathbb{P} = \mathbb{P}_{g_\theta}$ . However, due to the different expressions of optimization game, the training process (to the equilibrium point) for the MIM-based GAN is not the same as that for the original GAN, which is revealed by Eq. (5) and Eq. (7). Therefore, the differences between the two GANs may bring some novelties in theory and applications.*

## 2) Gradient of generator under the optimal discriminator:

With regard to the training process of GANs, it is worth discussing the gradient of objective function. Here, we intend to investigate the gradient of generator under the optimal discriminator, due to the fact that if the equilibrium is approximated, the discriminator is trained well already.

**Proposition 2.** *As for the MIM-based GAN, let  $g_\theta : \mathcal{Z} \rightarrow \mathcal{X}$  be a differentiable function which is used to generate data. When there exists the optimal discriminator  $D_{\text{MIM}}^*(\mathbf{x}) = \frac{1}{2} + \frac{1}{2} \ln \frac{P(\mathbf{x})}{P_{g_\theta}(\mathbf{x})}$ , the gradient*

function of the generator with respect to the parameter  $\theta$  is given by

$$\begin{aligned}
& \nabla_{\theta} \mathbb{E}_{\mathbf{z} \sim \mathbb{P}_z} [\exp(D_{MIM}^*(g_{\theta}(\mathbf{z})))] \\
&= \mathbb{E}_{\mathbf{z} \sim \mathbb{P}_z} \left[ \nabla_{\theta} \exp \left( \frac{1}{2} + \frac{1}{2} \ln \left( \frac{P(g_{\theta}(\mathbf{z}))}{P_{g_{\theta}}(g_{\theta}(\mathbf{z}))} \right) \right) \right] \\
&= \sqrt{e} \mathbb{E}_{\mathbf{z} \sim \mathbb{P}_z} \left[ \nabla_{\theta} \left( \frac{P(g_{\theta}(\mathbf{z}))}{P_{g_{\theta}}(g_{\theta}(\mathbf{z}))} \right)^{\frac{1}{2}} \right] \\
&= \frac{\sqrt{e}}{2} \mathbb{E}_{\mathbf{z} \sim \mathbb{P}_z} \left[ \left( \frac{P(g_{\theta}(\mathbf{z}))}{P_{g_{\theta}}(g_{\theta}(\mathbf{z}))} \right)^{-\frac{1}{2}} \frac{\nabla_{\theta} P(g_{\theta}(\mathbf{z})) P_{g_{\theta}}(g_{\theta}(\mathbf{z})) - \nabla_{\theta} P_{g_{\theta}}(g_{\theta}(\mathbf{z})) P(g_{\theta}(\mathbf{z}))}{P_{g_{\theta}}^2(g_{\theta}(\mathbf{z}))} \right) \right] \quad (11) \\
&= \frac{\sqrt{e}}{2} \mathbb{E}_{\mathbf{z} \sim \mathbb{P}_z} \left[ \frac{\nabla_{\theta} P(g_{\theta}(\mathbf{z})) \sqrt{\frac{P_{g_{\theta}}(g_{\theta}(\mathbf{z}))}{P(g_{\theta}(\mathbf{z}))}} - \nabla_{\theta} P_{g_{\theta}}(g_{\theta}(\mathbf{z})) \sqrt{\frac{P(g_{\theta}(\mathbf{z}))}{P_{g_{\theta}}(g_{\theta}(\mathbf{z}))}}}{P_{g_{\theta}}(g_{\theta}(\mathbf{z}))} \right].
\end{aligned}$$

**Remark 2.** As for the gradient of generator under the optimal discriminator, it is readily seen that when the generative data distribution is approximating the real data distribution, the gradient is getting small. That is to say, when the training state is close to the equilibrium, the training process is going to be over.

### 3) Anti-interference ability of generator:

Consider the fact that the discriminator makes a difference on the generator during the adversarial training process of GANs. Specifically, when there exists a disturbance in the discriminator, the generator will be drawn into the unstable training in some degree. Consequently, it is required to analyze the anti-interference ability of generator with respect to the disturbance in the discriminator.

**Proposition 3.** Let  $g_{\theta} : \mathcal{Z} \rightarrow \mathcal{X}$  be a differentiable function that induces a generative distribution  $\mathbb{P}_{g_{\theta}}$  for  $g_{\theta}(\mathbf{z})$ . Let  $\mathbb{P}_z$  be the distribution for  $\mathbf{z}$ ,  $\mathbb{P}$  be the real data distribution, as well as  $D$  be a discriminator ( $D \in [0, 1]$ ). Consider the stability for the gradient of generator in the MIM-based GAN in the two following cases.

- Assuming  $D - \tilde{D}^* = \epsilon$  ( $\epsilon$  denotes a small disturbance which satisfies  $\epsilon \in [0, 1]$ , as well as  $\tilde{D}^*$  is the ideal perfect discriminator i.e.  $\tilde{D}^*(g_{\theta}(\mathbf{z})) = 0$ ), we have

$$\begin{aligned}
\nabla_{\theta} \mathbb{E}_{\mathbf{z} \sim \mathbb{P}_z} [\exp(D(g_{\theta}(\mathbf{z})))] &= \mathbb{E}_{\mathbf{z} \sim \mathbb{P}_z} [\exp(D(g_{\theta}(\mathbf{z}))) \nabla_{\mathbf{x}} D(\mathbf{x}) \nabla_{\theta} g_{\theta}(\mathbf{z})] \\
&= \mathbb{E}_{\mathbf{z} \sim \mathbb{P}_z} [\exp(\tilde{D}^*(g_{\theta}(\mathbf{z})) + \epsilon) \nabla_{\mathbf{x}} D(\mathbf{x}) \nabla_{\theta} g_{\theta}(\mathbf{z})] \quad (12) \\
&= \exp(\epsilon) \mathbb{E}_{\mathbf{z} \sim \mathbb{P}_z} [\nabla_{\mathbf{x}} D(\mathbf{x}) \nabla_{\theta} g_{\theta}(\mathbf{z})].
\end{aligned}$$

- Assuming  $D - \check{D}^* = \epsilon$  ( $\epsilon$  is a small disturbance which satisfies  $|\epsilon| < \frac{1}{2}$ , as well as  $\check{D}^*$  is the worst

discriminator i.e.  $\check{D}^*(g_\theta(\mathbf{z})) = \frac{1}{2}$  implying that the training equilibrium is achieved), we have

$$\begin{aligned}\nabla_{\theta}\mathbb{E}_{\mathbf{z}\sim\mathbb{P}_z}[\exp(D(g_\theta(\mathbf{z})))]&= \mathbb{E}_{\mathbf{z}\sim\mathbb{P}_z}[\exp(\check{D}^*(g_\theta(\mathbf{z})) + \epsilon)\nabla_{\mathbf{x}}D(\mathbf{x})\nabla_{\theta}g_\theta(\mathbf{z})] \\ &= \exp\left(\frac{1}{2} + \epsilon\right)\mathbb{E}_{\mathbf{z}\sim\mathbb{P}_z}[\nabla_{\mathbf{x}}D(\mathbf{x})\nabla_{\theta}g_\theta(\mathbf{z})].\end{aligned}\quad (13)$$

**Corollary 1.** Let  $g_\theta : \mathcal{Z} \rightarrow \mathcal{X}$  be a differentiable function that is used to generate data following the distribution  $\mathbb{P}_{g_\theta}$ . Let  $\mathbb{P}_z$  be the distribution for  $\mathbf{z}$  ( $\mathbf{z} \in \mathcal{Z}$ ),  $\mathbb{P}$  be the real data distribution, and  $D$  be a discriminator ( $D \in [0, 1]$ ). Consider the condition satisfying  $D - \check{D}^* = \epsilon$  ( $\epsilon \in [0, 1]$  and  $\check{D}^*(g_\theta(\mathbf{z})) = 0$  denoting the ideal perfect discriminator) or  $D - \check{D}^* = \epsilon$  ( $|\epsilon| < \frac{1}{2}$  and  $\check{D}^*(g_\theta(\mathbf{z})) = \frac{1}{2}$  denoting the worst discriminator). In this regard, the gradient of generator in the MIM-based GAN has more anti-interference ability of generator than that in the original GAN.

*Proof.* According to the objective functions of MIM-based GAN, original GAN and its improved GAN, it is not difficult to see that the corresponding gradient functions of generators depend on  $\nabla_{\theta}\mathbb{E}_{\mathbf{z}\sim\mathbb{P}_z}[\exp(D(g_\theta(\mathbf{z})))]$ ,  $\nabla_{\theta}\mathbb{E}_{\mathbf{z}\sim\mathbb{P}_z}[\ln(1 - D(g_\theta(\mathbf{z})))]$  and  $\nabla_{\theta}\mathbb{E}_{\mathbf{z}\sim\mathbb{P}_z}[-\ln(D(g_\theta(\mathbf{z})))]$ , respectively.

On one hand, in the case that  $D - \check{D}^* = \epsilon$  ( $\epsilon \in [0, 1]$  and  $\check{D}^*(g_\theta(\mathbf{z})) = 0$ ), we have

$$\begin{aligned}\nabla_{\theta}\mathbb{E}_{\mathbf{z}\sim\mathbb{P}_z}[\ln(1 - D(g_\theta(\mathbf{z})))]&= \mathbb{E}_{\mathbf{z}\sim\mathbb{P}_z}\left[-\frac{\nabla_{\mathbf{x}}D(\mathbf{x})\nabla_{\theta}g_\theta(\mathbf{z})}{1 - D(g_\theta(\mathbf{z}))}\right] \\ &= \mathbb{E}_{\mathbf{z}\sim\mathbb{P}_z}\left[-\frac{\nabla_{\mathbf{x}}D(\mathbf{x})\nabla_{\theta}g_\theta(\mathbf{z})}{1 - \check{D}^*(g_\theta(\mathbf{z})) - \epsilon}\right] \\ &= -\frac{1}{1 - \epsilon}\mathbb{E}_{\mathbf{z}\sim\mathbb{P}_z}[\nabla_{\mathbf{x}}D(\mathbf{x})\nabla_{\theta}g_\theta(\mathbf{z})],\end{aligned}\quad (14)$$

$$\begin{aligned}\nabla_{\theta}\mathbb{E}_{\mathbf{z}\sim\mathbb{P}_z}[-\ln(D(g_\theta(\mathbf{z})))]&= \mathbb{E}_{\mathbf{z}\sim\mathbb{P}_z}\left[-\frac{\nabla_{\mathbf{x}}D(\mathbf{x})\nabla_{\theta}g_\theta(\mathbf{z})}{D(g_\theta(\mathbf{z}))}\right] \\ &= \mathbb{E}_{\mathbf{z}\sim\mathbb{P}_z}\left[-\frac{\nabla_{\mathbf{x}}D(\mathbf{x})\nabla_{\theta}g_\theta(\mathbf{z})}{\check{D}^*(g_\theta(\mathbf{z})) + \epsilon}\right] \\ &= -\frac{1}{\epsilon}\mathbb{E}_{\mathbf{z}\sim\mathbb{P}_z}[\nabla_{\mathbf{x}}D(\mathbf{x})\nabla_{\theta}g_\theta(\mathbf{z})].\end{aligned}\quad (15)$$

It is not difficult to see that  $\frac{1}{\epsilon}$  and  $\frac{1}{1-\epsilon}$  are symmetric in the case  $\epsilon \in [0, 1]$ , which implies that  $\nabla_{\theta}\mathbb{E}_{\mathbf{z}\sim\mathbb{P}_z}[-\ln(D(g_\theta(\mathbf{z})))]$  has the same anti-interference ability as  $\nabla_{\theta}\mathbb{E}_{\mathbf{z}\sim\mathbb{P}_z}[\ln(1 - D(g_\theta(\mathbf{z})))]$ .

As for the function  $h(u) = \frac{1}{1-u} - \exp(u)$  ( $u \in [0, 1]$ ), it is not difficult to see that  $h(u) \geq 0$  for  $u \in [0, 1]$  where the equation holds at  $u = 0$ . In fact,  $\exp(-u) \geq 1 - u$  for  $u \in [0, 1]$ . Therefore, by comparing Eq. (12) with Eq. (14) and Eq. (15), it is readily seen that the result of this corollary is true.

On the other hand, in the case that  $D - \check{D}^* = \epsilon$  ( $|\epsilon| < \frac{1}{2}$  and  $\check{D}^*(g_\theta(\mathbf{z})) = \frac{1}{2}$ ), it is not difficult to see that

$$\begin{aligned}\nabla_{\theta}\mathbb{E}_{\mathbf{z}\sim\mathbb{P}_z}[\ln(1 - D(g_\theta(\mathbf{z})))]&= \mathbb{E}_{\mathbf{z}\sim\mathbb{P}_z}\left[-\frac{\nabla_{\mathbf{x}}D(\mathbf{x})\nabla_{\theta}g_\theta(\mathbf{z})}{1 - \check{D}^*(g_\theta(\mathbf{z})) - \epsilon}\right] \\ &= -\frac{1}{\frac{1}{2} - \epsilon}\mathbb{E}_{\mathbf{z}\sim\mathbb{P}_z}[\nabla_{\mathbf{x}}D(\mathbf{x})\nabla_{\theta}g_\theta(\mathbf{z})],\end{aligned}\quad (16)$$

$$\begin{aligned}
\nabla_{\theta} \mathbb{E}_{z \sim \mathbb{P}_z} [-\ln(D(g_{\theta}(z)))] &= \mathbb{E}_{z \sim \mathbb{P}_z} \left[ -\frac{\nabla_x D(\mathbf{x}) \nabla_{\theta} g_{\theta}(z)}{\check{D}^*(g_{\theta}(z)) + \epsilon} \right] \\
&= -\frac{1}{\frac{1}{2} + \epsilon} \mathbb{E}_{z \sim \mathbb{P}_z} [\nabla_x D(\mathbf{x}) \nabla_{\theta} g_{\theta}(z)].
\end{aligned} \tag{17}$$

It is readily seen that  $\frac{1}{\frac{1}{2}-\epsilon}$  and  $\frac{1}{\frac{1}{2}+\epsilon}$  are symmetric if there exists a small disturbance, i.e.  $|\epsilon| < C < \frac{1}{2}$  ( $C$  is a constant), that is to say, the anti-interference ability for  $\nabla_{\theta} \mathbb{E}_{z \sim \mathbb{P}_z} [-\ln(D(g_{\theta}(z)))]$  is equal to that for  $\nabla_{\theta} \mathbb{E}_{z \sim \mathbb{P}_z} [\ln(1 - D(g_{\theta}(z)))]$ .

Considering the function  $h(u) = \frac{1}{\frac{1}{2}-u} - \exp(\frac{1}{2} + u)$  where  $u \in (-\frac{1}{2}, \frac{1}{2})$ , it is readily seen that  $h(u) > 0$  for  $u \in (-\frac{1}{2}, \frac{1}{2})$ . Thus, by comparing Eq. (13) with Eq. (16) and Eq. (17), it is easy to see that the result of this corollary also is true.

To sum up, the corollary is verified. □

**Remark 3.** *From the perspective of the gradient of generator, the disturbance in the discriminator is taken into a function to provide a multiplicative parameter for the gradient. In fact, the different gradients in the original GAN and MIM-based GAN are resulted from the different objective functions. Particularly, the exponential function in the gradient of MIM-based GAN is originated from the the partial derivative of its objective function with exponential one. While, the reciprocal function in the gradient of original GAN is derived from the logarithmic function of the objective function.*

### III. RARE EVENTS ANALYSIS IN GANS

From a new viewpoint to analyze GANs, we focus on the case that real data contains rare events and investigate how rare events make differences on the data generation and the corresponding applications of GANs.

#### A. Effect of rare events on generator

With respect to the training process of GANs, we usually train a pretty good discriminator and use it to lead the generator to reach its optimal objective function. Then, a better generator is also obtained to train the discriminator as a feedback. This process runs iteratively until reaches the equilibrium point. In this regard, if we have an optimal discriminator (an ideal case), our goal is to maximize the objective function by selecting an appropriate generator (according to Eq. (7)). In this case, relatively fewer occurrence events play minor roles in the objective function. This implies that the generator ignores smaller probability events (usually regarded as rare events) in some degree by maximizing the major part of objective function. As

a result, it is necessary to discuss the proportion of rare events in the objective functions of generators. Before this, we shall introduce a kind of rare events characterization to provide a specific example for rare events processing.

In general, rare events and large probability ones can be regarded to belong to two different classes, which implies there exists a binary distribution  $\{P(\bar{\Theta}), P(\Theta)\}$  where  $P(\bar{\Theta}) = p$  ( $p \ll \frac{1}{2}$ ) and  $P(\Theta) = 1 - p$  ( $\bar{\Theta}$  denotes the rare events and  $\Theta$  denotes the normal ones). For instance, in statistics, the minority set and majority set match this case. Specifically, the two sets satisfy

$$\begin{cases} \bar{\Theta} = \left\{ m_k \mid \left| \frac{m_k}{M} - p_k \right| \geq \xi, k = 1, 2, \dots, K \right\}, \\ \Theta = \left\{ m_k \mid \left| \frac{m_k}{M} - p_k \right| < \xi, k = 1, 2, \dots, K \right\}, \end{cases} \quad (18)$$

and the corresponding probability elements are given by

$$\begin{cases} P\{\bar{\Theta}\} \leq K \max_k P\left\{ \left| \frac{m_k}{M} - p_k \right| \geq \xi \right\} \leq \delta, \\ P\{\Theta\} = 1 - P\{\bar{\Theta}\} > 1 - \delta, \end{cases} \quad (19)$$

which results from the weak law of large numbers  $P\left\{ \left| \frac{m_k}{M} - p_k \right| < \xi \right\} > 1 - \delta$ , where  $m_k$  is the occurrence number of  $a_k$  (the sample support space is  $\{a_1, a_2, \dots, a_K\}$ ),  $p_k$  denotes a probability element from a distribution  $\{p, p_2, \dots, p_K\}$ ,  $M$  is the sample number, as well as  $0 < \xi \ll 1$  and  $0 < \delta \ll 1$ .

Based on the above discussion, we investigate how much proportion of rare events will be taken in the objective functions of GANs. This may reflect the rare events generation for the generator of GANs.

**Proposition 4.** *Let  $\mathbb{P}$  be the real data distribution involved with rare events, which is given by  $\mathbb{P} = \{p, 1-p\}$  ( $0 < p \ll \frac{1}{2}$ ) corresponding to the Eq. (19). Let  $g_\theta : \mathcal{Z} \rightarrow \mathcal{X}$  be a differentiable function to generate data which follows the distribution  $\mathbb{P}_{g_\theta}$  where  $\mathbb{P}_{g_\theta} = \{p + \varepsilon p^\gamma, 1 - p - \varepsilon p^\gamma\} = \{q, 1 - q\}$  ( $q < \frac{1}{2}$ ). Consider the case that the optimal discriminator is achieved, which implies  $D_{\text{MIM}}^*(\mathbf{x}) = \frac{1}{2} + \frac{1}{2} \ln \frac{P(\mathbf{x})}{P_{g_\theta}(\mathbf{x})}$  for the MIM-based GAN. In this case, the proportion of rare events in the objective function of generator is given by*

$$\Upsilon_{\text{MIM}} \approx \frac{\frac{p+q}{2} - \frac{1}{8}\varepsilon^2 p^{2\gamma-1}}{1 - \frac{1}{8}\varepsilon^2 \frac{p^{2\gamma-1}}{1-p}}, \quad (20)$$

where  $\varepsilon$  and  $\gamma$  denote a small disturbance parameter and an adjustable parameter (regarded as a constant) respectively.

*Proof.* In the light of the condition  $\mathbb{P}_{g_\theta} = \{p + \varepsilon p^\gamma, 1 - p - \varepsilon p^\gamma\} = \{q, 1 - q\}$  ( $q < \frac{1}{2}$ ), it is known that  $\varepsilon$  and  $\gamma$  represent the deviation between the two distributions  $\mathbb{P}$  and  $\mathbb{P}_{g_\theta}$ . Considering the optimal discriminator in the MIM-based GAN and the Eq. (7), it is readily seen that

$$\begin{aligned} L_{\text{MIM}}(D = D_{\text{MIM}}^*, G) &= \sqrt{e} \left\{ \mathbb{E}_{\mathbf{x} \sim \mathbb{P}} \left[ \left( \frac{P(\mathbf{x})}{P_{g_\theta}(\mathbf{x})} \right)^{-\frac{1}{2}} \right] + \mathbb{E}_{\mathbf{x} \sim \mathbb{P}_{g_\theta}} \left[ \left( \frac{P_{g_\theta}(\mathbf{x})}{P(\mathbf{x})} \right)^{-\frac{1}{2}} \right] \right\} \\ &= 2\sqrt{e} \left\{ p(1 + \varepsilon p^{\gamma-1})^{\frac{1}{2}} + (1-p) \left( 1 - \frac{\varepsilon p^\gamma}{1-p} \right)^{\frac{1}{2}} \right\}. \end{aligned} \quad (21)$$

Focusing on the rare events reflected into the probability element  $p$  rather than  $(1-p)$  ( $0 < p \ll \frac{1}{2}$ ), we have the proportion of rare events in the  $L_{\text{MIM}}(D = D_{\text{MIM}}^*, G)$  as follows

$$\begin{aligned} \Upsilon_{\text{MIM}} &= \frac{2\sqrt{e} \left\{ p(1 + \varepsilon p^{\gamma-1})^{\frac{1}{2}} \right\}}{L_{\text{MIM}}(D = D_{\text{MIM}}^*, G)} \\ &\stackrel{(a)}{=} \frac{p + \frac{1}{2}\varepsilon p^\gamma - \frac{1}{8}\varepsilon^2 p^{2\gamma-1} + o(\varepsilon^2)}{\left\{ p + \frac{1}{2}\varepsilon p^\gamma - \frac{1}{8}\varepsilon^2 p^{2\gamma-1} + o(\varepsilon^2) \right\} + \left\{ (1-p) - \frac{1}{2}\varepsilon p^\gamma - \frac{1}{8}\varepsilon^2 \frac{p^{2\gamma}}{1-p} + o(\varepsilon^2) \right\}} \\ &= \frac{\frac{p+q}{2} - \frac{1}{8}\varepsilon^2 p^{2\gamma-1} + o(\varepsilon^2)}{1 - \frac{1}{8}\varepsilon^2 \frac{p^{2\gamma-1}}{1-p} + o(\varepsilon^2)} \\ &\approx \frac{\frac{p+q}{2} - \frac{1}{8}\varepsilon^2 p^{2\gamma-1}}{1 - \frac{1}{8}\varepsilon^2 \frac{p^{2\gamma-1}}{1-p}}, \end{aligned} \quad (22)$$

where the equality (a) is derived from Taylor's theorem.  $\square$

**Corollary 2.** Let  $\mathbb{P}$  and  $\mathbb{P}_{g_\theta}$  be the real data distribution and generative data distribution, where  $\mathbb{P} = \{p, 1-p\}$  ( $0 < p \ll \frac{1}{2}$ ) and  $\mathbb{P}_{g_\theta} = \{p + \varepsilon p^\gamma, 1 - p - \varepsilon p^\gamma\} = \{q, 1 - q\}$  ( $q < \frac{1}{2}$ ). Consider the case that the optimal discriminator is achieved, which implies  $D_{\text{MIM}}^*(\mathbf{x}) = \frac{1}{2} + \frac{1}{2} \ln \frac{P(\mathbf{x})}{P_{g_\theta}(\mathbf{x})}$  for the MIM-based GAN and  $D_{\text{KL}}^*(\mathbf{x}) = \frac{P(\mathbf{x})}{P(\mathbf{x}) + P_{g_\theta}(\mathbf{x})}$  for the original GAN. In this regard, compared with the original GAN, the MIM-based GAN usually maintains higher proportion of rare events in the objective function of generator, namely  $\Upsilon_{\text{MIM}} \geq \Upsilon_{\text{KL}}$ , where the equality is hold in the case  $p = q$ .

*Proof.* Similar to Proposition 4, as for the rare events analysis in the original GAN, we have

$$\begin{aligned} L_{\text{KL}}(D = D_{\text{KL}}^*, G) &= \mathbb{E}_{\mathbf{x} \sim \mathbb{P}} \left[ \ln \frac{P(\mathbf{x})}{P(\mathbf{x}) + P_{g_\theta}(\mathbf{x})} \right] + \mathbb{E}_{\mathbf{x} \sim \mathbb{P}_{g_\theta}} \left[ \ln \frac{P_{g_\theta}(\mathbf{x})}{P(\mathbf{x}) + P_{g_\theta}(\mathbf{x})} \right] \\ &= -p \ln(2 + \varepsilon p^{\gamma-1}) - (1-p) \ln(2 - \varepsilon \frac{p^\gamma}{1-p}) \\ &\quad + p(1 + \varepsilon p^{\gamma-1}) \ln(1 - \frac{1}{2 + \varepsilon p^{\gamma-1}}) + (1-p - \varepsilon p^\gamma) \ln(1 - \frac{1}{2 - \varepsilon \frac{p^\gamma}{1-p}}), \end{aligned} \quad (23)$$

in which the the proportion of rare events is given by

$$\begin{aligned}
\Upsilon_{\text{KL}} &= \frac{-p \ln(2 + \varepsilon p^{\gamma-1}) + p(1 + \varepsilon p^{\gamma-1}) \ln(1 - \frac{1}{2 + \varepsilon p^{\gamma-1}})}{L_{\text{KL}}(D = D_{\text{KL}}^*, G)} \\
&= \frac{\frac{p+q}{2} - \frac{1}{8 \ln 2} \varepsilon^2 p^{2\gamma-1} + o(\varepsilon^2)}{1 - \frac{1}{8 \ln 2} \varepsilon^2 \frac{p^{2\gamma-1}}{1-p} + o(\varepsilon^2)} \\
&\approx \frac{\frac{p+q}{2} - \frac{1}{8 \ln 2} \varepsilon^2 p^{2\gamma-1}}{1 - \frac{1}{8 \ln 2} \varepsilon^2 \frac{p^{2\gamma-1}}{1-p}}.
\end{aligned} \tag{24}$$

According to  $p < \frac{1}{2}$  and  $q < \frac{1}{2}$ , we have  $\frac{p+q}{2(1-p)} < 1$ . Then, it is not difficult to see that the term of right-hand side in Eq. (22) is larger than that in Eq. (24), which verifies the proposition.  $\square$

**Remark 4.** Consider that the objective function guides the generator networks of GANs to generate fraudulent fake data. Since the dominant component of objective function depends on larger probability events, a generator prefers to output the data belonging to the normal data set. In order to reveal the ability of rare events generation for generators, it is significant to compare the rare events proportion in different objective functions, which is discussed in Proposition 4 and Corollary 2. Furthermore, according to Proposition 3 and Corollary 1, it is implied that when there exists some disturbance for rare events, the MIM-based GAN still keeps more stable than the original GAN, which means the former has more anti-interference ability to generate rare events. To sum up, it is reasonable that the MIM-based GAN performs more efficient than the original GAN on rare events generation.

### B. GAN-based anomaly detection

As a promising application of GANs, anomaly detection has attracted much attention of researchers. According to the principle of GANs, it is known that by resorting to the Nash equilibrium of objective function rather than a single optimization, the generator gains more representative power and specificity to represent the real data. Actually, to identify anomalies (belonging to rare events) with GANs, the outputs of generator network are regarded to approximate normal events. Then, by use of identification tools such as Euclidean distance, anomalies are detected due to their evident differences from the generative events (corresponding to normal ones). Simultaneously, a trained discriminator network is also used to dig out the anomalies not in the generative data.

Due to the similar principle between the original GAN and MIM-based GAN, the anomaly detection method is not only suitable for the former but also for the latter. In this regard, we will introduce how to build a data processing model based on GANs (such as the original GAN and the MIM-based GAN), and how to use it to identify anomalous events (hardly ever appearing in the training data) in details.

### 1) Procedure for anomaly detection with GANs:

Here, a procedure of GAN-based detection shall be introduced, which provides a general framework for different GANs to detect anomalies (where we take the MIM-based GAN as an example). Our main goal is to assign labels  $\{0, 1\}$  (“0” for normal events and “1” for anomalous ones) to testing samples. The details are given as follows.

- **Step 1: data processing preparation with GANs**

At first, we generate some fake data similar to the real data by use of GAN. By feeding training data  $x$  and the random data  $z$  in the latent space to the MIM-based GAN model, we train the generator and discriminator (both based on neural networks) with the two-player maxmin game given by Eq. (4) to obtain the generative data.

- **Step 2: anomaly score computing**

In this step, a detection measurement tool named anomaly score is designed based on the generative data and the corresponding GANs. After enough training iterations, we have the trained discriminator  $D$  and generator  $G$  and then make use of them jointly to identify the anomalous events by means of the anomaly score which is introduced in Section III-B2.

- **Step 3: decision for detection**

By using anomaly scores of the testing samples (obtained in the step 2) to make a decision for detection, we label each sample in the testing dataset as

$$A^{\text{test}} = \begin{cases} 1, & \text{for } S^{\text{test}} > \Gamma, \\ 0, & \text{otherwise,} \end{cases} \quad (25)$$

where  $A^{\text{test}}$  is a label for a testing sample, whose non-zero value indicates a detected rare event, i.e. the anomaly score is higher than a predefined threshold  $\Gamma$ .

### 2) Anomaly score based on both discriminator and generator:

The superiority of architecture of GANs is that we jointly train two neural networks, namely the discriminator and the generator, which makes one more decision tool available. We would like to exploit both discriminator and generator as tools to dig out anomalies. In fact, there are two parts in the GAN-based anomaly detection as follows.

- **Generator-based anomaly detection**

In terms of the trained generator  $G$  which generates realistic samples, it is regarded as a mapping from a latent data space to the real data space, namely  $G : \mathcal{Z} \rightarrow \mathcal{X}$ . Since that it is more likely to learn the

normal data which occurs frequently, the generator tends to reflect the principal components of the real data' distribution. In this regard, the generator is also considered as an inexplicit model to reflect the normal events. Considering the smooth transitions in the latent space, we have the similar outputs of generator when the inputs are close enough in the latent space. Furthermore, if we can find the latent data  $\mathbf{z}$  which is the most likely mapped into the testing data  $\mathbf{x}$ , the similarity between testing data  $\mathbf{x}$  and reconstructed testing data  $G(\mathbf{z})$  reveals how much extent  $\mathbf{x}$  can be viewed as a sample drawn from the distribution reflected by  $G$ . As a result, it is applicable to use the residuals between  $\mathbf{x}$  and  $G(\mathbf{z})$  to identify the anomalous events hidden in testing data. In addition, we should also consider the discriminator loss as a regularization for the residual loss, which ensures the reconstructed data  $G(\mathbf{z})$  to lie on the manifold  $\mathcal{X}$ .

- **Discriminator-based anomaly detection**

The trained discriminator  $D$  which distinguishes generative data from real data with high sensitivity, is a direct tool to detect the anomalies.

Considering GAN-based anomaly detection, it is the most important to find the optimal  $\mathbf{z}$  in the latent space, which is mapped to the testing samples approximately. In this regard, a random  $\mathbf{z}$  from the latent space is chosen and put into the generator to produce the reconstructed sample  $G(\mathbf{z})$  which corresponds to the sample  $\mathbf{x}$ . Then, we update  $\mathbf{z}$  in the latent space by means of gradient descent with respect to the loss function given by Eq. (27). After sufficient iteration (namely the loss function hardly ever decreasing), we gain the most likely latent data  $\mathbf{z}$  mapped into the testing data, which means the optimal  $\mathbf{z}_{\text{opt}}$  is obtained by

$$\mathbf{z}_{\text{opt}} = \arg \min_{\mathbf{z}} J_{\text{error}}(\mathbf{x}, \mathbf{z}), \quad (26)$$

where the loss function  $J_{\text{error}}(\mathbf{x}, \mathbf{z})$  is given by

$$J_{\text{error}}(\mathbf{x}, \mathbf{z}) = (1 - \lambda) \|\mathbf{x} - G(\mathbf{z})\|_p + \lambda H_{\text{ce}}(D(G(\mathbf{z})), \beta), \quad (27)$$

in which  $\lambda$  is an adjustable weight ( $0 < \lambda < 1$ ),  $\|\cdot\|_p$  denotes the  $p$ -norm (usually  $p = 2$ ), and  $H_{\text{ce}}(\cdot, \cdot)$  denotes the sigmoid cross entropy which is given by

$$H_{\text{ce}}(D(G(\mathbf{z})), \beta) = -\beta \ln \left[ \frac{1}{1 + \exp(-D(G(\mathbf{z})))} \right] - (1 - \beta) \ln \left[ 1 - \frac{1}{1 + \exp(-D(G(\mathbf{z})))} \right], \quad (28)$$

with the target  $\beta = 1$ .

Furthermore, by combining the  $J_{\text{error}}(\mathbf{x}, \mathbf{z})$  and  $D(\mathbf{x})$ , we have the anomaly detection loss, referred to as *anomaly score*, which is given by

$$S^{\text{test}} = (1 - \eta)J_{\text{error}}(\mathbf{x}, \mathbf{z}_{\text{opt}}) + \eta H_{\text{ce}}(D(\mathbf{x}), \beta), \quad (29)$$

where the adjustable weight satisfies  $0 < \eta < 1$ , as well as,  $\beta = 1$ .

In view of the above descriptions, the outputs of trained discriminator and generator are exploited to calculate a set of anomaly scores for test data. Then, we detect the anomalies by use of the decision-making tool described as Eq. (25).

### 3) Analysis for the anomaly detection with GANs:

Here, we shall discuss the intrinsic principle of the above anomaly detection method. Specifically, we take the detection method with the MIM-based GAN as an example to give some analyses. Considering that the anomaly score (as a main part in the detection method) consists of two parts related to GANs, we will analyze the corresponding two parts, respectively, as follows.

- **Analysis for generator-based detection:** As for the generator  $G$  which maps the latent samples into realistic samples, it tends to generate the data with large probability in the real data set. Specifically, if we classify the real data into the large probability events set  $\Omega_{\text{large}}$  and the small probability events (or rare events) set  $\Omega_{\text{rare}}$ , we will have the proportion of large probability events in the objective function mentioned in Eq. (3) as follows

$$\begin{aligned} R_{\Omega_{\text{large}}} &= \frac{\int_{\Omega_{\text{large}}} [P(\mathbf{x}) \exp(1 - D(\mathbf{x})) + P_{g_\theta}(\mathbf{x}) \exp(D(\mathbf{x}))] d\mathbf{x}}{\int_{\Omega_{\text{large}} + \Omega_{\text{rare}}} [P(\mathbf{x}) \exp(1 - D(\mathbf{x})) + P_{g_\theta}(\mathbf{x}) \exp(D(\mathbf{x}))] d\mathbf{x}} \\ &\stackrel{(b)}{=} \frac{\int_{\Omega_{\text{large}}} \left[ P(\mathbf{x}) \left( \frac{P(\mathbf{x})}{P_{g_\theta}(\mathbf{x})} \right)^{-\frac{1}{2}} + P_{g_\theta}(\mathbf{x}) \left( \frac{P_{g_\theta}(\mathbf{x})}{P(\mathbf{x})} \right)^{-\frac{1}{2}} \right] d\mathbf{x}}{\int_{\Omega_{\text{large}} + \Omega_{\text{rare}}} \left[ P(\mathbf{x}) \left( \frac{P(\mathbf{x})}{P_{g_\theta}(\mathbf{x})} \right)^{-\frac{1}{2}} + P_{g_\theta}(\mathbf{x}) \left( \frac{P_{g_\theta}(\mathbf{x})}{P(\mathbf{x})} \right)^{-\frac{1}{2}} \right] d\mathbf{x}} \\ &= \frac{\int_{\Omega_{\text{large}}} [P(\mathbf{x}) P_{g_\theta}(\mathbf{x})]^{\frac{1}{2}} d\mathbf{x}}{\int_{\Omega_{\text{large}} + \Omega_{\text{rare}}} [P(\mathbf{x}) P_{g_\theta}(\mathbf{x})]^{\frac{1}{2}} d\mathbf{x}}, \end{aligned} \quad (30)$$

where the equality (b) is obtained by substituting the optimal  $D_{\text{MIM}}^*$  (mentioned in Eq. (5)) into the discriminator  $D$ . When the generative probability  $P_{g_\theta}(\mathbf{x})$  is close to the real probability  $P(\mathbf{x})$ , we have  $P_{g_\theta}(\mathbf{x}) \approx P(\mathbf{x}) \gg 0$  in the region  $\{\mathbf{x} \in \Omega_{\text{large}}\}$ , while in the region  $\{\mathbf{x} \in \Omega_{\text{rare}}\}$ ,  $P_{g_\theta}(\mathbf{x})$  is pretty small or even approximates to zero. In this case, the proportion of large probability events in the objective function approximates to the probability of large probability events, namely  $R_{\Omega_{\text{large}}} \approx$

$$\frac{\int_{\Omega_{\text{large}}} P(\mathbf{x}) d\mathbf{x}}{\int_{\Omega_{\text{large}} + \Omega_{\text{rare}}} P(\mathbf{x}) d\mathbf{x}} = \int_{\Omega_{\text{large}}} P(\mathbf{x}) d\mathbf{x} \rightarrow 1. \text{ This implies that the generative data } G(\mathbf{z}) \text{ is more likely to}$$

belong to the large probability events set (which is usually the main part of normal events), regarded as the whole of normal events. It is readily seen that large probability events set make more effects on training the generator than rare events set (which usually consists of the small part of normal events with smaller probability and anomalous events). Furthermore, in the loss function  $J_{\text{error}}(\mathbf{x}, \mathbf{z})$ ,  $\|\mathbf{x} - G(\mathbf{z})\|_p$  is minimized to let  $\mathbf{x}$  be close to a generative event (regarded as a normal event), while  $H_{\text{ce}}(D(G(\mathbf{z})), \beta)$  enforces  $G(\mathbf{z})$  to be in the real data space. As a result, large enough  $J_{\text{error}}(\mathbf{x}, \mathbf{z})$  usually reflect the anomalous events, which plays an important role in the anomaly score.

- **Analysis for discriminator-based detection:** As the second term of anomaly score,  $H_{\text{ce}}(D(\mathbf{x}), \beta)$  is based on a well trained discriminator (similar to the optimal one). In terms of the ideal discriminator as Eq. (5), it can make a decision whether a sample belongs to the training data set (namely the real data set) or not. In particular, when a testing data does not appear in the training data set, the corresponding value of  $D(\mathbf{x})$  approximates to zero (which implies a large cross entropy). While, the values of  $D(\mathbf{x})$  for other testing data (included in the training data set) are more likely close to  $\frac{1}{2}$ . In this regard, the discriminator is exploited for anomaly detection.

**Remark 5.** *It is necessary to give comparisons for the original GAN and MIM-based GAN to detect anomalies. Due to the similar two-player game principle, the original GAN and MIM-based GAN have analogous characteristics in the anomaly detection. However, from the discussion of Corollary 2, we know that the MIM-based GAN pays more attention to the small part of normal events (which are with smaller probability) in some degree than the original GAN. In other words, the smaller probability events in the normal events set are more likely generated rather than lost, which indicates that the regarded anomalous events set is more close to the real anomalous events set and contains less normal events with small probability. This has a positive impact on the anomaly detection.*

#### IV. EXPERIMENTS

Now, we present experimental results to show the efficiency of MIM-based GAN and other classical GANs. Particularly, we compare our method with other adversarial networks (such as the original GAN, LSGAN and WGAN) with respect to data generation and anomaly detection. Our main findings for the MIM-based GAN may be that:

- Compared with some classical GANs, training performance improvements are available during the training process to the equilibrium;

- By use of MIM-based GAN, there exists the better performance on detecting anomalies than other classical GANs.

### A. Datasets

As far as the datasets are concerned, artificial data and real data are considered to compare different approaches and evaluate their performance. Particularly, on one hand, we take artificial Gaussian distribution data as an example, whose mean and standard deviation are denoted by  $\mu$  and  $\sigma$  respectively. In this regard, the Gaussian distribution  $\mathcal{N}(\mu, \sigma)$  can be chosen arbitrarily such as  $\mathcal{N}(\mu = 4, \sigma = 1.25)$ . On the other hand, several online real datasets (including the MNIST dataset and Outlier Detection DataSet (ODDS)) are also investigated, whose details are listed as follows.

- **MNIST:** As for this dataset, 10 different classes of digits  $\{0, 1, 2, \dots, 9\}$  in MNIST are generated by use of GANs. In order to apply this case into anomaly detection, we choose one kind of digit class (such as “0”) as the rare events (namely anomalies), while the rest parts are treated as normal ones. In other words, there exist 10% rare events mixed in the whole dataset. The training set consists of 60,000 image samples ( $28 \times 28$  pixel gray handwritten digital images), while there are 10,000 image samples in the testing set.
- **ODDS:** Considering that it is necessary to process real-world datasets in practice, we shall investigate several anomaly detection datasets from the ODDS repository as follows.
  - Cardiotocography:* The Cardiotocography dataset in ODDS repository has 21 features in each sample, such as Fetal Heart Rate (FHR) and Uterine Contraction (UC) features. As a classification dataset with 1,831 samples, the pathologic class is regarded as the anomalous events class including 176 samples (9.6% contamination).
  - Thyroid:* The Thyroid dataset is obtained from the UCI machine learning repository, which contains 6 real attributes (namely features). Its goal is to determine whether a patient referred to the clinic is hypothyroid, which is viewed as a kind of anomaly detection. In this database, there are 3,772 samples, including 93 hyperfunction samples (2.5% anomalous events) which make up the minority class.
  - Musk:* The Musk dataset in ODDS repository consists of 3,062 samples including 3.2% anomalies. Specifically, the dataset contains several-musks and non-musk classes, which are regarded as the inliers and outliers (or anomalies) respectively. By the way, there exist 166 features in each sample.

## B. Experiment details

### 1) Experiment for training performance comparison:

In order to intuitively give some comparisons on the training performances of GANs, we use the artificial data following Gaussian distribution  $\mathcal{N}(\mu = 4, \sigma = 1.25)$  to train the MIM-based GAN, original GAN (based on KL divergence), LSGAN (based on Least Squares distance) and WGAN (based on Wasserstein distance) with Pytorch.

In particular, we first train the adversarial networks for some iterations (such as 500, 1,000 and 1,500 training iterations) to obtain a not bad discriminator. During each iteration, there are 16,000 samples produced by programming as initial input data for the discriminator. Then, with the fixed discriminator, a generator is trained by reducing the error of objective function in each kind of adversarial networks. Furthermore, we adopt two Deep Neural Networks (DNNs) as the discriminator and generator, in which the Stochastic Gradient Descent (SGD) optimizer with 0.001 learning rate is chosen and the activation functions of discriminator and generator are sigmoid and tanh function respectively. Finally, we draw the error curves of the objection functions of generators to show the different performance during the training process.

### 2) Anomaly detection experiment based on MNIST and ODDS:

When detecting anomalies in the MNIST and ODDS, we adopt the general framework of GANs described in Section III-B1. However, to compare the efficiency of different GANs, including the original GAN, MIM-based GAN, LSGAN and WGAN, we change the main part (namely different objective functions for the data generation) of the framework. Based on the imbalanced datasets, the Receiver Operating Characteristic (ROC) curve, Area Under Curve (AUC) and  $F_1$ -score are used as criterions to compare different GANs for anomaly detection.

In details, the detection procedure on the MNIST and ODDS is similar to that mentioned in Section III-B1, where the neural networks training of GANs is the key point. At first, as for the framework of neural networks, DNNs are used, whose activation functions in the output layers are sigmoid function and tanh function for the discriminator and generator respectively and those in the other layers are all leaky ReLU. Moreover, the Adam algorithm is chosen to optimize the weights for the networks with 0.001 learning rate. According to the properties of MNIST and ODDS, we configure the hidden layer size 256 for the MNIST and Musk dataset (belonging to the ODDS) as well as 64 for the Cardiotocography and Thyroid in the ODDS. Furthermore, when we obtain trained GANs and the corresponding generative data,

we use Eq. (27) and Eq. (29) (where  $\lambda = 0.1$  and  $\eta = 0.05$ ) to gain anomaly scores for testing data, in which the optimal  $z_{\text{opt}}$  in latent space is obtained by used of Adam optimizer with learning rate 0.003. At last, we adopt Eq. (25) to label the testing data so that the outliers (namely anomalies) are detected.

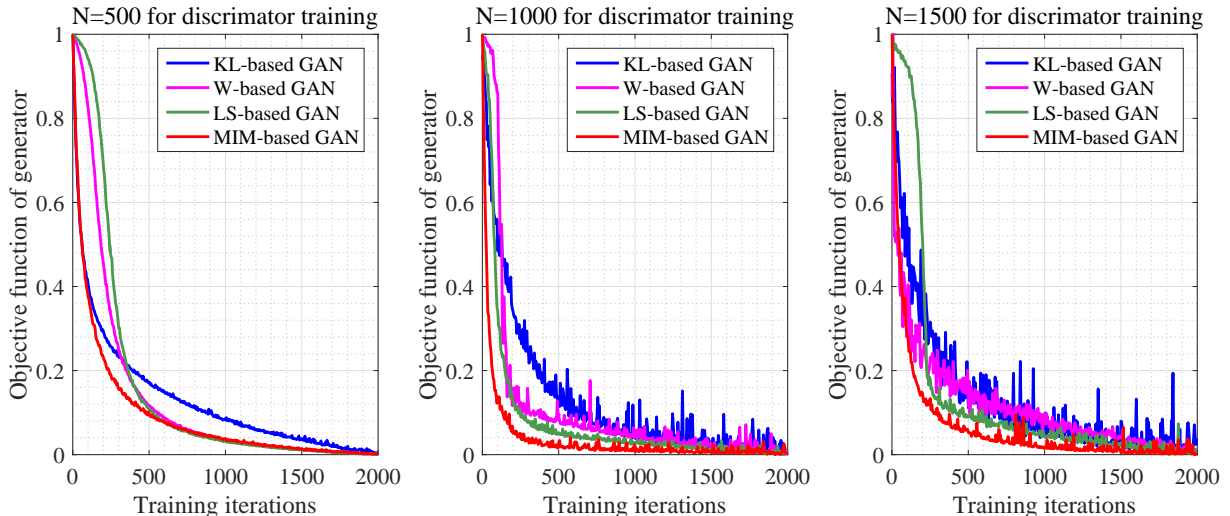


Fig. 1. The MIM-based GAN, original GAN (or KL-based GAN), LSGAN (or LS-based GAN) and WGAN (or W-based GAN) are used to generate the samples following Gaussian distribution  $\mathcal{N}(\mu = 4, \sigma = 1.25)$  where  $\mu$  and  $\sigma$  denotes the mean and the standard deviation respectively. There are 16,000 input samples following the Gaussian distribution in each training iteration. The generators are trained with the discriminators fixed for 500, 1,000 or 1,500 training iterations (namely  $N = 500, 1,000$  or  $1,500$ ). In these cases, the curves for the objection functions of generators are drawn to compare the performances on training process.

### C. Results and discussion

According to the above design for experiments, we do simulations with Pytorch and Matlab to evaluate the theoretical analysis. In particular, the experiment results are discussed as follows.

#### 1) Training performance of GANs:

From figure 1, it is illustrated that during the training process, the MIM-based GAN, LSGAN and WGAN all perform better than the original GAN in the aspects of convergence and stability of training process. While, the MIM-based GAN also has its own superiority. On one hand, the objective function in the MIM-based GAN goes to zero more quickly than that in the other GANs, even with not too many iterations on the discriminator. On the other hand, when a discriminator is given, the training stability of generator for MIM-based GAN performs better than that for original GAN, which is also comparable to that for LSGAN and WGAN. In brief, the MIM-based GAN converges to equilibrium faster and

more stably than the original GAN. It also has these advantages on the training process to some degree, compared with LSGAN and WGAN.

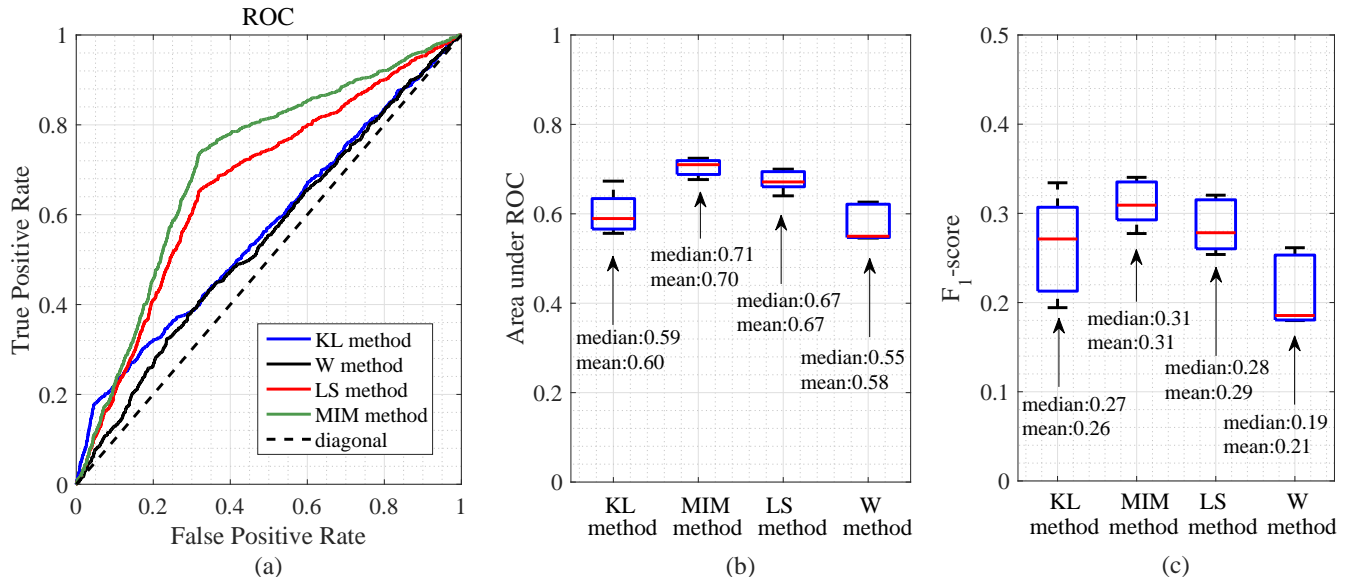


Fig. 2. The MIM-based GAN, original GAN (or KL-based GAN), LSGAN (or LS-based GAN) and WGAN (or W-based GAN) are used to generate the data similar to the MNIST with 30 training iterations. The samples labeled digit “0” in the MNIST are chosen as the anomalous events where there are 60,000 training samples and 10,000 testing samples in the MNIST. By using the framework described in Section III-B1 to detect the anomalous events in the testing dataset, the ROC curve of detection results is shown (as subfigure (a)), as well as, AUC and  $F_1$ -score are drawn (as subfigures (b) and (c)) with 20 experiments to provide the performance comparison for the different GAN-based detection approaches.

## 2) Results of anomaly detection for MNIST and ODDS:

Figure 2 shows the performance of anomaly detection with different GANs in the MNIST experiment, including ROC curve, AUC and  $F_1$ -score. In general, it is not difficult to see that the MIM-based GAN improves these kinds of performance compared with the other GANs. This is resulted from the fact that MIM-based objective function enlarges the proportion of rare events. Moreover, we also see that the volatility of the detection results (shown by the AUC and  $F_1$ -score) in the KL-based GAN and W-based GAN methods is greater than that in two other methods.

Figure 3, 4 and 5 compare the different GAN-based detection methods in the case of ODDS by showing the performances in terms of ROC curve, AUC and  $F_1$ -score. Although there exists different performance in the different kinds of datasets of ODDS, MIM-based GAN still possesses advantages on the anomaly detection. Particularly, on one hand, the ROC curve for MIM-based GAN method is more approximate

to the ideal standard than that for the other detection methods with GANs. On the other hand, as for the AUC and  $F_1$ -score of detection results, the corresponding statistics (including the median and mean) performs better when using MIM-based GAN method as shown in the box-plots (b) and (c) in Figure 3, 4 and 5. Actually, these datasets from ODDS repository provide some convincing and realistic evidences for the advantage of MIM-based GAN on anomaly detection.

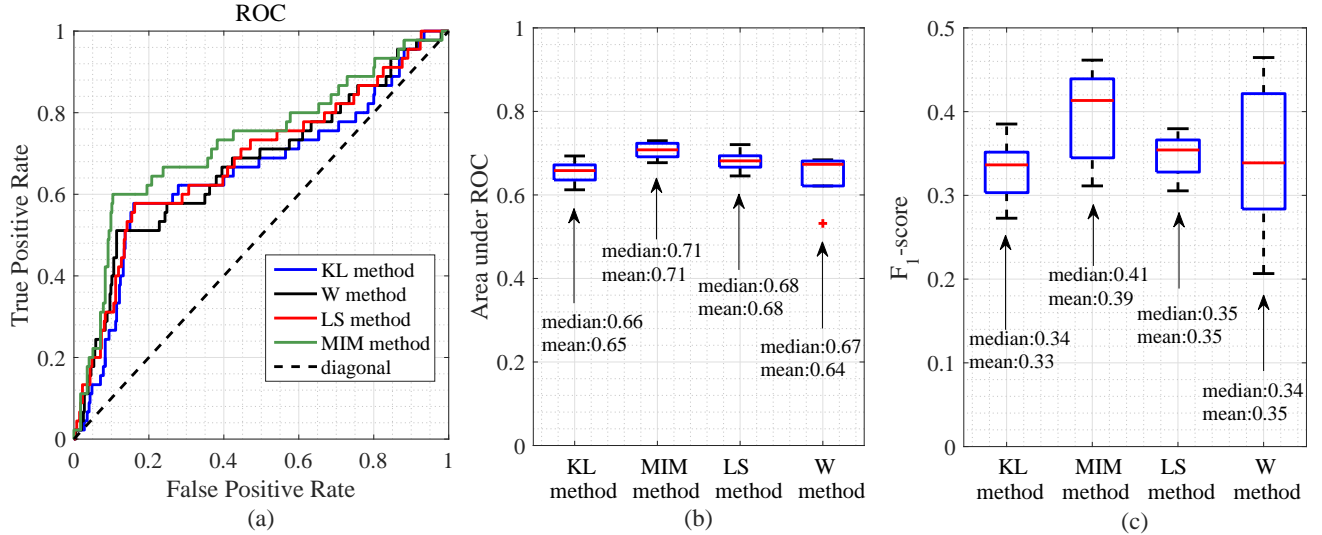


Fig. 3. The MIM-based GAN, original GAN, LSGAN and WGAN are used to generate the data similar to the Cardiotocography dataset (which belongs to the ODDS). After randomly shuffling the data, we use 1,360 samples (about 74.28% data) as the input samples to train the GANs (with 500 training iterations) and the rest are treated as the testing samples for the detection procedure. In order to compare the performance of the different GAN-based approaches, the ROC curve, AUC and  $F_1$ -score are drawn (as subfigures (a), (b) and (c)) with 20 experiments in this figure.

## V. CONCLUSION

In this paper, we proposed a new approach deemed MIM-based GAN, an alternative to the conventional GANs. In terms of this new model, it has different performance of training process with the other classical GANs. Furthermore, another advantage of this new developed approach is to highlight the proportion of rare events in the objective function to generate more efficient data. In addition, we showed that compared with the classical GANs, the MIM-based GAN has more superiority on the anomaly detection, which may be a promising application direction with GANs in practice.

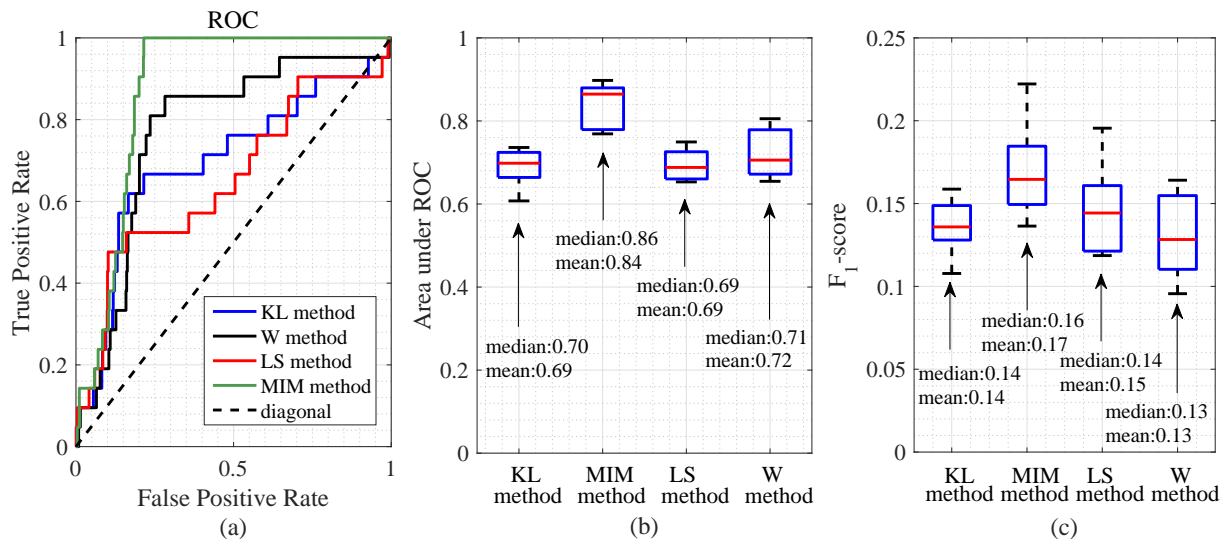


Fig. 4. Considering the anomaly detection on the Thyroid dataset (a kind of dataset in the ODDS), we use 2800 samples (about 74.23% data) as training samples for the the MIM-based GAN, original GAN, LSGAN and WGAN (whose training iterations are all 500). Then, the rest samples are treated as the testing samples. To intuitively compare the detection results of different GAN-based methods, the ROC curve, AUC and  $F_1$ -score are drawn (as box-plots (a), (b) and (c)) with 20 experiments.

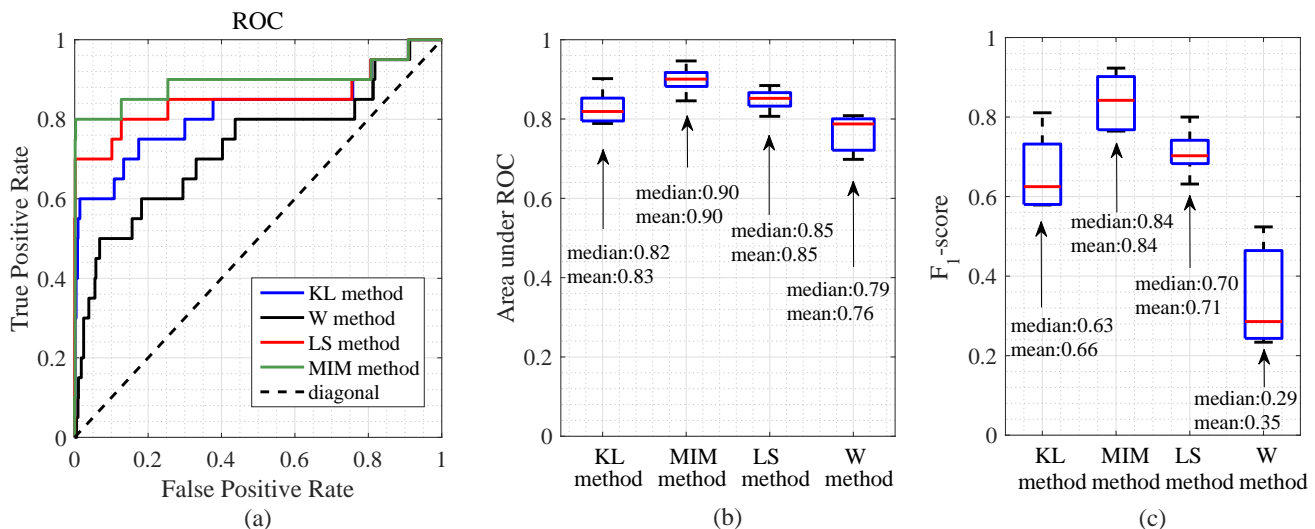


Fig. 5. To generate data similar to the Musk dataset, the MIM-based GAN, original GAN, LSGAN and WGAN are used with 2,200 training samples (about 71.85% data) where the number of training iterations is 20. The rest samples are regarded as testing samples for these GAN-based detection methods. To show detection results intuitively, the ROC curve is given (as subfigure (a)), as well as, AUC and  $F_1$ -score are drawn (as subfigures (b) and (c)) with 20 experiments in this figure.

#### ACKNOWLEDGMENT

We thank a lot for the advices from Prof. Xiaodong Wang and Xiao-Yang Liu at Columbia University, USA. Their suggestions make a positive effect on this work. Meanwhile, we also appreciate the visiting

scholar experience supported by Tsinghua Scholarship for Overseas Graduate Studies.

## REFERENCES

- [1] I. J. Goodfellow, J. Pouget-Abadie, M. Mirza, B. Xu, D. Warde-Farley, S. Ozair, A. Courville and Y. Bengio, “Generative adversarial nets”, in *Proc. Advances in Neural Information Processing Systems (NeurIPS 2014)*, Montreal, Quebec, Canada, Dec. 8–13, 2014, pp. 2672–2680.
- [2] X. Mao, Q. Li, H. Xie, R. Lau, Z. Wang, and S. P. Smolley, “On the effectiveness of least squares generative adversarial networks,” *IEEE Trans. Pattern Anal. Mach. Intell.*, vol. 41, no. 12, pp. 2947–2960, Dec. 2019.
- [3] S. Wang, G. Peng, and Z. Zheng, “Capturing joint label distribution for multi-label classification through adversarial learning,” *IEEE Trans. Knowl. Data Eng.*, vol. 14, no. 8, pp. 1–12, Aug. 2015.
- [4] Y. Liu, Z. Li, C. Zhou, Y. Jiang, J. Sun, M. Wang and X. He “Generative adversarial active learning for unsupervised outlier detection,” *IEEE Trans. Knowl. Data Eng.*, early access, pp. 1–12, 2019.
- [5] T. Fernando, S. Denman, S. Sridharan, and C. Fookes, “Memory augmented deep generative models for forecasting the next shot location in tennis,” *IEEE Trans. Knowl. Data Eng.*, early access, pp. 1–12, 2019.
- [6] C. Ledig, L. Theis, F. Huszar, J. Caballero, A. P. Aitken, A. Tejani, J. Totz, Z. Wang and W. Shi, “Photo-realistic single image super-resolution using a generative adversarial network”, in *Proc. IEEE Conference on Computer Vision and Pattern Recognition (CVPR 2017)*, Honolulu, HI, USA, Jul. 21–26, 2017, pp. 4681–4690.
- [7] A. Kuefler, J. Morton, T. A. Wheeler and M. J. Kochenderfer, “Imitating driver behavior with generative adversarial networks”, in *Proc. IEEE Intelligent Vehicles Symposium (IV 2017)*, Los Angeles, CA, USA, Jun. 11–14, 2017, pp. 204–211.
- [8] A. Shrivastava, T. Pfister, O. Tuzel, J. Susskind, W. Wang and R. Webb, “Learning from simulated and unsupervised images through adversarial training”, in *Proc. IEEE Conference on Computer Vision and Pattern Recognition (CVPR 2017)*, Honolulu, HI, USA, Jul. 21–26, 2017, pp. 2107–2116.
- [9] C. K. Sonderby, J. Caballero, L. Theis, W. Shi and F. Huszar, “Amortised map inference for image super-resolution”, in *Proc. International Conference on Learning Representations (ICLR 2017)*, Palais des Congres Neptune, Toulon, France, Apri. 24–26, 2017, pp. 1–17.
- [10] J. Zhao, M. Mathieu and Y. LeCun, “Energy-based generative adversarial networks”, in *Proc. International Conference on Learning Representations (ICLR 2017)*, Palais des Congres Neptune, Toulon, France, Apri. 24–26, 2017, pp. 1–16.
- [11] X. Mao, Q. Li, H. Xie, R. Y. K. Lau, Z. Wang and S. P. Smolley, “Least squares generative adversarial networks”, in *Proc. IEEE International Conference on Computer Vision (ICCV 2017)*, Venice, Italy, Oct. 22–29, 2017, pp. 2794–2802.
- [12] Y. Mroueh and T. Sercu, “Fisher GAN”, in *Proc. Advances in Neural Information Processing Systems (NeurIPS 2017)*, Long Beach, CA, USA, Dec. 3–9, 2017, pp. 2513–2523.
- [13] S. Nowozin, B. Cseke and R. Tomioka, “f-GAN: Training generative neural samplers using variational divergence minimization”, in *Proc. Advances in Neural Information Processing Systems (NeurIPS 2016)*, Barcelona, Spain, Dec. 5–10, 2016, pp. 271–279.
- [14] M. Arjovsky, S. Chintala and L. Bottou, “Wasserstein GAN”, <https://arxiv.org/abs/1701.07875>, pp. 1–32.
- [15] I. Gulrajani, F. Ahmed, M. Arjovsky, V. Dumoulin and A. Courville, “Improved training of Wasserstein GANs”, in *Proc. Advances in Neural Information Processing Systems (NeurIPS 2017)*, Long Beach, CA, USA, Dec. 3–9, 2017, pp. 5767–5777.
- [16] H. Soleimani and D. J. Miller, “ATD: Anomalous topic discovery in high dimensional discrete data,” *IEEE Trans. Knowl. Data Eng.*, vol. 28, no. 9, pp. 2267–2280, Sep. 2016.
- [17] M. Radovanovic, A. Nanopoulos, and M. Ivanovic, “Reverse nearest neighbors in unsupervised distance-based outlier detection,” *IEEE Trans. Knowl. Data Eng.*, vol. 27, no. 5, pp. 1369–1382, May. 2015.

- [18] C. Oreilly, A. Gluhak, and M. A. Imran, “Adaptive anomaly detection with kernel eigenspace splitting and merging,” *IEEE Trans. Knowl. Data Eng.*, vol. 27, no. 1, pp. 3–16, Jan. 2015.
- [19] D. Li, D. Che, J. Goh, and S. Ng. “Anomaly detection with generative adversarial networks for multivariate time series”, in *Proc. ACM Knowledge Discovery and Data Mining Conference Workshops (KDD Wkshps 2018)*, London, United Kingdom, Aug. 19–23, 2018, pp. 1–10.
- [20] L. Deecke, R. Vandermeulen, L. Ruff, S. Mandt, and M. Kloft, “Image anomaly detection with generative adversarial networks”, in *Proc. Joint European Conference on Machine Learning and Knowledge Discovery in Databases (ECML-PKDD 2018)*, Dublin, Ireland, Sep. 10–14, 2018, pp. 3–17.
- [21] T. Schlegl, P. Seebock, S. M. Waldstein, U. Schmidt-Erfurth, and G. Langs, “Unsupervised anomaly detection with generative adversarial networks to guide marker discovery”, in *Proc. International Conference on Information Processing in Medical Imaging (IPMI 2017)*. Boone, North Carolina, USA, Jun. 25–30, 2017, pp. 146–157.
- [22] M. Ravanbakhsh, E. Sangineto, M. Nabi, and N. Sebe, “Training adversarial discriminators for cross-channel abnormal event detection in crowds”, in *Proc. IEEE Winter Conference on Applications of Computer Vision (WACV 2019)*, Hawaii, United States, Jan. 7–11, 2019, pp. 1896–1904.
- [23] H. Zenati, C. S. Foo, B. Lecouat, G. Manek, and V. R. Chandrasekhar, “Adversarially learned anomaly detection”, in *Proc. IEEE International Conference on Data Mining (ICDM 2018)*, Singapore, Singapore, Nov. 17–20, 2018, pp. 727–736.
- [24] P. Isola, J. Y. Zhu, T. Zhou and A. A. Efros, “Image-to-image translation with conditional adversarial networks,” in *Proc. IEEE Conference on Computer Vision and Pattern Recognition (CVPR 2017)*, Honolulu, HI, USA, Jul. 21–26, 2017, pp. 1125–1134.
- [25] J. Donahue, P. Krahenbuhl, and T. Darrell, “Adversarial feature learning”, in *Proc. International Conference on Learning Representations (ICLR 2017)*, Palais des Congres Neptune, Toulon, France, Apri. 24–26, 2017, pp. 1–18.
- [26] T. Schlegl, P. Seebock, S. M. Waldstein, G. Langs and U. Schmidt-Erfurth, “f-AnoGAN: Fast unsupervised anomaly detection with generative adversarial networks”, *Medical Image Analysis*, vol. 54, pp. 30–44, May 2019.
- [27] A. Odena, V. Dumoulin and C. Olah. “Deconvolution and checkerboard artifacts”, *Distill*, vol. 1, no. 10, Oct, 17, 2016, <http://distill.pub/2016/deconv-checkerboard>
- [28] D. Lopez-Paz and M. Oquab. “Revisiting classifier two-sample tests”, in *Proc. International Conference on Learning Representations (ICLR 2017)*, Palais des Congres Neptune, Toulon, France, Apri. 24–26, 2017, pp. 1–15.
- [29] P. Fan, Y. Dong, J. X. Lu, and S. Y. Liu, “Message importance measure and its application to minority subset detection in big data”, in *Proc. IEEE Globecom Workshops (GC Wkshps 2016)*, Washington D.C., USA, Dec. 4–8, 2016, pp. 1–6.
- [30] S. Liu, R. She, and P. Fan, “Differential message importance measure: A new approach to the required sampling number in big data structure characterization”, *IEEE Access*, vol. 6, pp. 42851–42867, Jul. 2018.
- [31] S. Liu, R. She, P. Fan, and K. B. Letaief. “Non-parametric message important measure: Storage code design and transmission planning for big data”, *IEEE Trans. Commun.*, vol. 66, no. 11, pp. 5181–5196, Nov. 2018.
- [32] R. She, S. Y. Liu, and P. Fan, “Amplifying inter-message distance: On information divergence measures in big data”, *IEEE Access*, vol. 5, pp. 24105–24119, Nov. 2017.